Determination of the thickness of Al_2O_3 barriers in magnetic tunnel junctions

J. D. R. Buchanan,[a] T. P. A. Hase, and B. K. Tanner
Department of Physics, South Road, University of Durham, Durham, DH1 3LE. United Kingdom

N. D. Hughes and R. J. Hicken
School of Physics, Stocker Road, University of Exeter, Exeter, EX4 4QL. United Kingdom

(Received 6 February 2002; accepted for publication 29 May 2002)

The barrier thickness in magnetic spin-dependent tunnel junctions with Al_2O_3 barriers has been measured using grazing incidence x-ray reflectivity and by fitting the tunneling current to the Simmons model. We have studied the effect of glow discharge oxidation time on the barrier structure, revealing a substantial increase in Al_2O_3 thickness with oxidation. The greater thickness of barrier measured using grazing incidence x-ray reflectivity compared with that obtained by fitting current density–voltage to the Simmons electron tunneling model suggests that electron tunneling is localized to specific regions across the barrier, where the thickness is reduced by fluctuations due to nonconformal roughness. © *2002 American Institute of Physics.* [DOI: 10.1063/1.1496131]

Magnetic Tunnel junctions (MTJs) consist of two ferromagnetic layers separated by a thin insulating layer that exhibits magnetoresistance (MR) due to spin polarized tunneling.[1] Since the discovery of tunneling magnetoresistance (TMR), at room temperature in oxide based barrier MTJs, this effect has been an intense area of research. Indeed, TMR devices such as these show a great deal of potential in the field of magnetic read heads found in hard disk drives and magnetic random access memory.[2]

MTJs are routinely fabricated with an Al_2O_3 barrier, through the plasma oxidation of an initially deposited Al layer. The barrier properties play a key role in the magnetotransport behavior[3–5] and so, to date, much attention has been paid to the study of these properties and their evolution throughout the fabrication process. The barriers are known to contain defects, some natural[6] and others of artificial origin.[7,8] Factors such as the barrier roughness[9] and chemical homogeneity[10] have been investigated as well as the specifics of barrier oxidation.[11,12]

It is important in the optimization of TMR to understand the oxidation process and in particular how to oxidize the entire Al layer and none of the ferromagnet.[13,14] We have measured the thickness of the insulating Al_2O_3 barriers, with varying oxidation times, using grazing incidence x-ray techniques and compared results gained from fitting current density–voltage ($I-V$) curves to an electron tunneling model. It has already been noted that the ''effective'' or ''characteristic'' thickness found with this approach differs greatly from more direct structural characteristic methods such as high-resolution electron microscopy.[12,15] However, due to the limiting field of view, it is difficult to accurately determine the averaged thickness and roughness over the sample. In this letter, we quantitatively compare the barrier thickness determined by structural and electrical methods.

The MTJs were deposited by dc sputtering of successive layers of cobalt, aluminum, and permalloy ($Ni_{81}Fe_{19}$) through shadow masks onto a silicon (100) substrate previously coated with rf sputtered aluminum oxide. The initial base pressure was 1×10^{-7} Torr and the sputtering was conducted in an argon atmosphere of 5 mTorr.

A Dektak profilometer was used to calibrate the Al deposition rate; a rate of $6.7(\pm0.1)$ Å/s was established. A standard Al layer thickness of 14 Å was used in all samples by exposing the sample to the Al source for 2.1 s via a timed shutter. Immediately after the Al layer was deposited, 100 mTorr of oxygen was introduced into the chamber and the sample was exposed to a localized dc glow discharge for 1 to 5 min (an additional unoxidized control sample was also made). The chamber was then pumped out to regain base pressure before the $Ni_{81}Fe_{19}$ layer was deposited. The nominal uncalibrated structure for each sample was Si(100)/250 Å Al_2O_3/90 Å Co/14 Å Al barrier/110 Å NiFe.

A quartz crystal oscillator system continuously recorded the deposition rate revealing that the $Ni_{81}Fe_{19}$ and Co layers in all samples were the same within $\pm5\%$. The crystal monitors were insufficiently sensitive to determine the thickness and errors of the Al layers, but the reproducible results for the Co and $Ni_{81}Fe_{19}$ gave confidence that the Al layers were the same thickness within $\pm5\%$ for all the samples. The standard deposited Al layer was $14(\pm0.7)$ Å.

A four-point dc measurement technique was used to determine both the magnetoresistance (MR) response and the $I-V$ characteristics. The height and width of the insulating barrier was determined by fitting the $I-V$ curve to a model based on the work of Simmons[16–18] as modified by Hartman.[19] The model uses the Wentzel–Kramers–Brillouin approximation, which assumes a slowly varying potential compared with the electron wavelength. The model takes into account the trapezoidal barrier shape caused by the differing work functions of the two metals, the effect of the image charge potential and is extended for use at room temperature.

Grazing incidence x-ray reflectivity (GIXR) measure-

[a] Author to whom correspondence should be addressed; electronic mail: j.d.r.buchanan@durham.ac.uk

 © 2002 American Institute of Physics
Downloaded 21 Apr 2011 to 129.234.252.66. Redistribution subject to AIP license or copyright; see http://apl.aip.org/about/rights_and_permissions

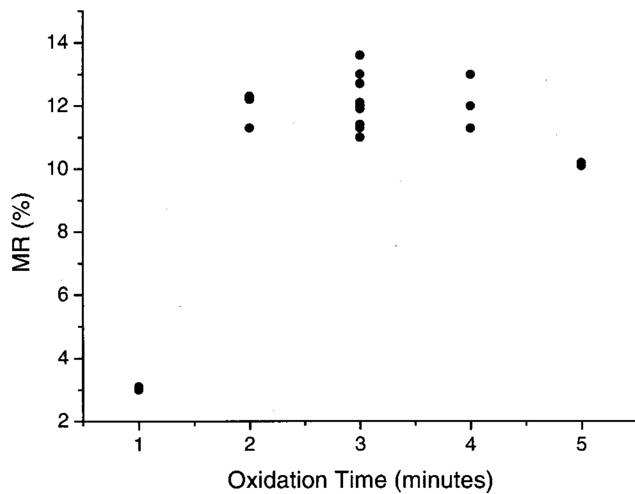

FIG. 1. The variation in MR with individual MTJ as a function of the oxidation time of the aluminum oxide barrier.

ments were made on a *Bede GXR1* reflectometer in the Durham laboratory. The true specular profile provided in-plane averaged structural information as a function of depth, such as layer thickness and interface width. This technique is ideally suited to the characterization of Al_2O_3 barriers in MTJ due to the large difference in scattering factors between the barrier and the surrounding ferromagnetic layers. However, simulations of model reflectivity profiles show that this technique can not be used to distinguish between Al and Al_2O_3 in MTJs, and so it is impossible to determine directly the degree of Al oxidation using GIXR.

An initial series of 21 MTJs with a nominal preoxidized Al thickness of 14 Å were grown in order to explore the relationship between MR and oxidation time. The results are shown in Fig. 1; a peak in the MR coincides with a three min oxidation period, indicating this to be the optimum oxidation. A smaller oxidation period leads to samples with lower MR, probably due to portions of the Al barrier being unoxidized, resulting in pinhole formation and the presence of other high conductivity regions. The lower MR with greater oxidation times is explained through the partial oxidation of the lower magnetic Co layer.

TABLE I. Structural parameters used to fit specular data, seen in Fig. 2, for a MTJ with a 5 min barrier oxidation period.

Layer	Thickness (Å)	Roughness (Å)
Si	⋯	6.5 ± 0.5
Al_2O_3	239 ± 5	3.4 ± 0.5
Co	124 ± 5	4.5 ± 0.5
Al_2O_3	31.2 ± 1	2.3 ± 0.5
NiFe	153 ± 5	2.1 ± 0.5
Oxide	3.1 ± 2	6.8 ± 0.5

The barrier widths were determined through fits to the $I-V$ data taken in a bias voltage range of ±700 mV as shown in the Fig. 2 inset (bias destruction tests revealed a mean breakdown voltage of 1.1 V). As a direct comparison, samples oxidized for 1, 3, and 5 min have been characterized using GIXR. An example of the specular reflectivity profile with the corresponding fit to a model structure has been shown in Fig. 2. The specular data have been corrected for the effect of forward diffuse scatter (also shown) by subtraction of the intensity measured in a similar $\theta/2\theta$ scan but with the specimen offset by $-0.1°$ from the specular condition. Data fitting having been performed using the BEDE MERCURY code.[20] This program uses a genetic algorithm to achieve a best fit between the data and that simulated for a model structure under the distorted wave born approximation. The structural parameters used in modeling the fit in Fig. 2 can be seen in Table I.

The metallic layer thickness and roughness values were found to be similar for all samples, demonstrating consistency and good control throughout the sputtering process. Values for the interface width between the Co and the Al_2O_3 barrier (4.5 Å) make an interesting comparison to the interface between the Al and the Co in the nonoxidized sample. This sample, as well as others[21,22] show a larger interface width of 8 ± 1 Å. This suggests the oxidation process results in the migration of the Al out of the Co layer. Both GIXR and $I-V$ modeling show a monotonic increase in barrier width with oxidation time, see Fig. 3 and Table II.

The most dramatic observation noted from the GIXR results is that the oxide barrier thickness is, in all cases,

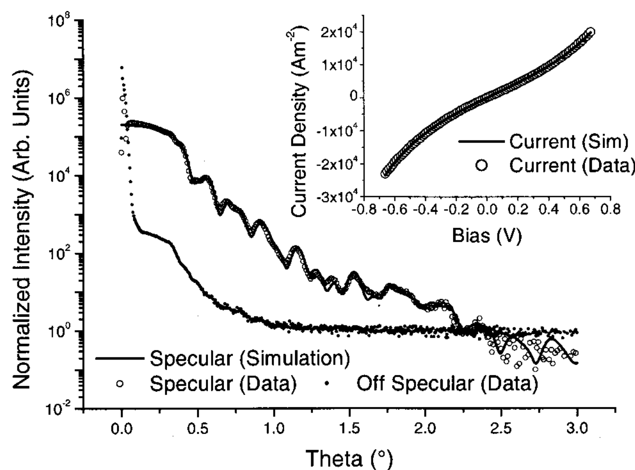

FIG. 2. True Specular (data and fit) and offspecular profile for a MTJ with a 5 min barrier oxidation period. The inset shows the typical data and corresponding fit for the $I-V$ Simmon's modeling.

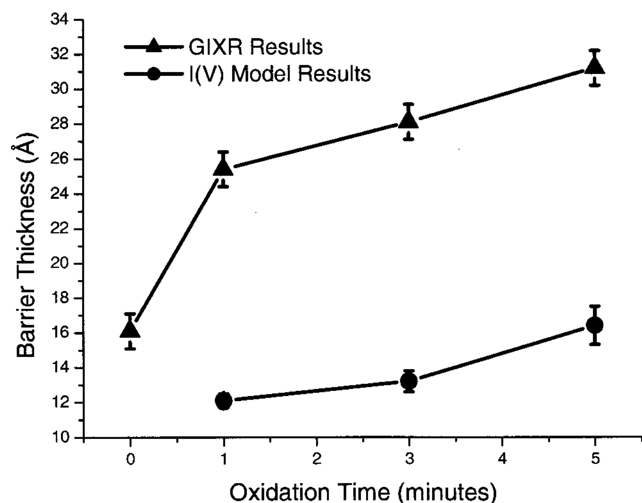

FIG. 3. A measure of barrier thickness as a function of oxidation time using (i) GIXR and (ii) $I-V$ Simmons modeling.

Downloaded 21 Apr 2011 to 129.234.252.66. Redistribution subject to AIP license or copyright; see http://apl.aip.org/about/rights_and_permissions

TABLE II. Measured barrier thickness for different oxidation times using (i) GIXR and (ii) $I-V$ Simmons modeling.

Sample oxidation	Thickness (Å)			Ratio of GIXR and $I-V$ thickness	MR (%)
	Nominal	GIXR	$I-V$		
None	14	16.1	⋯	⋯	⋯
1 min	14	25.4	12.1	2.1	3.1
3 min	14	28.1	13.2	2.1	12.1
5 min	14	31.2	16.4	1.9	10.2

much greater than the thickness of the initial Al layer and twice that of the value determined from the $I-V$ modeling. This result has been found for all the oxidized samples; the barrier thickness from the $I-V$ modeling was close to that of the Al layer prior to oxidation. The result is not an artifact of the GIXR modeling process as measurement of the Al layer thickness of the unoxidized control sample yielded a value of $16.1(\pm 1)$Å, in excellent agreement with the Dektak profilometer calibration. (The sensitivity is such that changing the barrier thickness by 5 Å results in a dramatically different reflectivity profile.)

Increased barrier width with oxidation has been reported previously by other groups[12,15] using physical characterization techniques, with the values obtained from the Simmons model being close to the nominal thickness expected from the preoxidized Al thickness. However, Schuller *et al.*[23,24] have shown that $I-V$ modeling is unreliable for evaluation of the barrier quality.

The present results show definitively that the effective or characteristic thickness obtained from the tunneling model does not correspond to the average thickness determined from GIXR. The absence of Kiessig fringes in the longitudinal offspecular diffuse scatter in Fig. 2 shows that there is almost zero conformality between the roughness of the top and bottom surfaces. The absence of fringes of the appropriate period implies that the roughness is thus nonconformal across the barrier layers. Transverse diffuse scans were taken with soft x rays at 780 eV to determine the in-plane correlation length from the half width of the diffuse scatter. There is only a small variation in correlation length; $\xi = 330 \pm 20$ Å for the unoxidized and 5 min oxidized sample, with the 1 and 3 min oxidized samples indicating a lower correlation length of less than 300 Å. This analysis thus indicates considerable local variation in the barrier thickness due to roughness, the discrepancy between effective ($I-V$) and average (GIXR) barrier thickness being explained by localized tunneling at areas in which the barrier thickness is near a minimum. If this is the case, $I-V$ modeling will always measure the lower thickness values for barriers compared to the average values obtained from GIXR.

Da Costa *et al.*[9] used an atomic force microscope equipped with a conducting tip to compare topographical information with current flow. Their results showed large local variations in the tunneling current which were attributed to small changes in barrier thickness and barrier potential, and so confirm that total conductance is dominated by contributions from localized sites.

In summary, we have found an oxidation time of 3 min produces sputtered MTJs with the highest MR values. The barrier thickness measured by fitting $I-V$ curves to the Simmons electron-tunneling model and by GIXR has been observed to increase monotonically as a function of oxidation time. GIXR results yield an average thickness much greater than that inferred from fitting the $I-V$ data and show a lack of conformality in the roughness. We understand that the discrepancy in thickness measured by the two techniques is supported by independent evidence.[25] These data quantify earlier indications that tunneling is localized to specific regions across the barrier where the barrier thickness is at a minimum.

The authors gratefully acknowledge financial support from EPSRC, partially through the (G&T)MR Network. One of the authors (B.K.T.) thanks the Leverhulme Trust for the award of a Research Fellowship.

[1] J. S. Moodera, L. R. Kinder, T. M. Wong, and R. Meservey, Phys. Rev. Lett. **74**, 3273 (1995).
[2] S. S. P. Parkin, K. P. Rocke, M. G. Samant, P. M. Rice, R. B. Beyers, R. E. Scheuerlein, E. J. O'Sullivan, S. L. Brown, J. Bucchigano, D. W. Abraham, L. Yu, M. Rooks, P. L. Trouilloud, R. A. Wanner, and W. J. Gallagher, J. Appl. Phys. **85**, 5828 (1999).
[3] J. C. Slonczewski, Phys. Rev. B **39**, 6995 (1989).
[4] J. M. MacLaren, X. G. Zhang, and W. H. Butler, Phys. Rev. B **56**, 11827 (1997).
[5] J. Mathon, Phys. Rev. B **56**, 11810 (1997).
[6] C. H. Shang, J. Nowak, R. Jansen, and J. S. Moodera, Phys. Rev. B **58**, R2917 (1998).
[7] R. Jansen and J. S. Moodera, J. Appl. Phys. **83**, 6682 (1998).
[8] E. Y. Tsymbal and D. G. Pettifor, J. Appl. Phys. **85**, 5801 (1999).
[9] V. Da Costa, F. Bardou, C. Béal, Y. Henry, J. P. Bucher, and K. Ounadjela, J. Appl. Phys. **83**, 6703 (1998).
[10] R. C. Sousa, J. J. Sun, V. Soares, P. P. Freitas, A. Kling, M. F. da Silva, and J. C. Soares, Appl. Phys. Lett. **73**, 3288 (1998).
[11] J. S. Moodera, E. F. Gallagher, K. Robinson, and J. Nowak, Appl. Phys. Lett. **70**, 3050 (1997).
[12] T. E. Clark, F. B. Mancoff, S. X. Wang, M. B. Clemens, and R. Sinclair, IEEE Trans. Magn. **35**, 2922 (1999).
[13] J. Nassar, M. Hehn, A. Vaures, F. Petroff, and A. Fert, Appl. Phys. Lett. **73**, 698 (1998).
[14] M. Sato, H. Kikuchi, and K. Koayashi, J. Appl. Phys. **83**, 6691 (1998).
[15] P. Shang, A. Petford-Long, J. H. Nickel, M. Sharma, and T. C. Anthony, J. Appl. Phys. **89**, 6874 (2001).
[16] J. G. Simmons, J. Appl. Phys. **34**, 1793 (1963).
[17] J. G. Simmons, J. Appl. Phys. **34**, 2581 (1963).
[18] J. G. Simmons, J. Appl. Phys. **35**, 2655 (1964).
[19] T. E. Hartman, J. Appl. Phys. **35**, 3283 (1964).
[20] M. Wormington, C. Pannacione, K. M. Matney, and D. K. Bowen, Philos. Trans. R. Soc. London, Ser. A **357**, 2827 (1999).
[21] J. D. R. Buchanan, T. P. A. Hase, B. K. Tanner, P. J. Chen, L. Gan, C. J. Powell, and W. F. Egelhoff, Jr. (unpublished).
[22] W. F. Egelhoff, P. J. Chen, R. D. McMichael, C. J. Powell, R. D. Deslattes, F. G. Serpa, and R. D. Gomez, J. Appl. Phys. **89**, 5209 (2001).
[23] B. Jönsson-Åkerman, R. Escudero, C. Leighton, S. Kim, I. K. Schuller, and D. A. Rabson, Appl. Phys. Lett. **77**, 1870 (2000).
[24] J. J. Åkerman, J. M. Slaughter, R. W. Dave, and I. K. Schuller, Appl. Phys. Lett. **79**, 3104 (2001).
[25] Ivan Schuller and Chris Leighton (private communication).

Downloaded 21 Apr 2011 to 129.234.252.66. Redistribution subject to AIP license or copyright; see http://apl.aip.org/about/rights_and_permissions